Removal of histone tails from nucleosome dissects the physical mechanisms of salt-induced aggregation, linker histone H1-induced compaction and 30-nm fiber formation of the nucleosome array.

Kohji Hizume[1], Tonau Nakai[2], Sumiko Araki[3], Eloise Prieto[1], Kenichi Yoshikawa[3] and Kunio Takeyasu[1] *

[1]*Laboratory of Plasma Membrane and Nuclear Signaling, Graduate School of Biostudies, Kyoto University, Yoshida Konoe-cho, Sakyo-ku, Kyoto, 606-8501, Japan*

[2]*Department of Mechanical and Aerospace Engineering, Graduate School of Engineering, Tottori University4-101 Koyama-minami, Tottori, 680-8552, Japan*

[3]*Department of Physics, Graduate School of Science, Kyoto University, Kitashirakawa-oiwake-cho, Sakyo-ku, Kyoto, 606-8502, Japan*

* Corresponding Auther **Postal address** Yoshida Konoe-cho, Sakyo-ku, Kyoto, 606-8502, Japan, **Tel/FAX** +81-75-753-6852, **e-mail address** takeyasu@lif.kyoto-u.ac.jp,

PACS codes keywords

Abstract

In order to reveal the roles of histone tails in the formation of higher-order

chromatin structures, we employed atomic force microscopy (AFM), and an *in vitro*

reconstitution system to examine the properties of reconstituted chromatin

composed of tail-less histones and a long DNA (106-kb plasmid) template. The

tail-less nucleosomes did not aggregate at high salt concentrations or with an

excess amount of core histones, in contrast with the behavior of nucleosomal arrays

composed of nucleosomes containing normal, N-terminal tails. Analysis of our

nucleosome distributions reveals that the attractive interaction between tail-less

nucleosomes is weakened. Addition of linker histone H1 into the tail-less

nucleosomal array failed to promote the formation of 30 nm chromatin fibers that

are usually formed in the normal nucleosomal array. These results demonstrate

that the attractive interaction between nucleosomes via histone-tails plays a

critical role in the formation of the uniform 30-nm chromatin fiber.

1. Introduction

The structural unit of the eukaryotic chromosome is the nucleosome [1,2], which is a nucleoprotein structure composed of about 146 bp of DNA wrapped around a core histone octamer [3]. Nucleosomes interact with each other, leading to the formation of higher-order organizational structures. These different chromatin structures are believed to play a key role in the regulation of various genomic events by modulating the accessibility of specific regions of genomic DNA to transcriptional protein complexes [4-6].

The attractive interaction between nucleosomes is enhanced by high concentrations of salt [7-9] and chromosomal proteins such as linker histone H1 [10,11], HMG (High Mobility Group) proteins [12], and transcriptional regulators. Many chromosomal proteins induce aggregation of nucleosomes, however only linker histone H1 has been observed to convert an array of nucleosomes into a well-organized 30-nm fiber [13,14].

The core histone amino-terminus, or "histone-tail", has been thought to be a significant factor in the higher-order arrangement of the nucleosomal array [15]. All of the four core histones carry the amino-terminal tail regions, which are rich in lysine residues. These tails spread out of the nucleosome core [3], and undergo post-transcriptional modifications such as acetylation, phosphorylation, and methylation [16-18]. Trypsin digestion leads to the loss of these nucleosome tails,

and analysis of AFM images of the nucleosomal array with tail-less histone H3 has shown that the H3-tail-less nucleosomes are arranged in a "zig-zag" manner by the addition of linker histone H5, as normal nucleosomes do [19,20].

AFM has been applied to the structural analysis of chromatin [13,19-33], because of its ability to to reveal chromatin structures with the nm-scale resolution and its less requirement for sample preparation (in principle, special staining and fixation are not necessary). For a biochemical system in combination with the AFM analysis, we have developed an efficient *in vitro* chromatin reconstitution system with 100 kb plasmid DNA and core histones isolated from HeLa cells [25,27]. Using this system, we have reconstructed the step-wise folding assembly of a nucleosome array from 11 nm 'beads-on-a-string' to 30 nm fibers with the help of histone H1 [13]. In this study, we analyzed the structure of the nucleosome array both with and without histone-tails and in the presence or absence of linker histones, and dissected the effect that histone-tail removal has on the step-wise chromatin folding process.

2. Materials and Methods.

DNA and histones

The 100 kb plasmid (pBAC7/8-α2) employed in the chromatin reconstitution was a kind gift from Dr. Ikeno at Fujita Health University, Japan [34], and has been used in previous studies [13,27,29,30]. This plasmid was constructed as follows: First, the 25 kb alphoid fragment (tandem repeats of 171 bp unit of alphoid DNA from the centromeric region of the human 21st chromosome [35]) was isolated from the cosmid clone, Q25F12, obtained from the LL21NC02 library (Lawrence Livermore Laboratory) by *SfiI* digestion and cloned into the *SfiI* site of pBAC-TAN that had been created by the insertion of a *MluI-SfiI-SacII* linker into the *XhoI* site of pBeloBAC11. Then, the resultant alphoid-BAC, which contained 100 kb of tandem alphoid insert (4 repeats of the 25 kb fragment), was digested with *MluI* and *SacII*, and the *MulI-SacII* fragment was subcloned into the *SalI* site of pBAC-108L [36] resulting in the 100 kb plasmid, pBAC7/8-α2.

Core histones were purified from HeLa cells according to the method developed by T. E. O'Neill et al. [37] with slight modifications. The cells were harvested, washed with PBS, and then lysed with L-buffer [140 mM NaCl, 10 mM Tris-Cl (pH 7.5), and 0.5 % Triton-X100]. Nuclei were isolated by low-speed centrifugation and washed three times with W-buffer [350 mM NaCl, 10 mM Tris-Cl (pH 7.5)]. The nuclei were then treated with micrococcal nuclease (40

units/mg of DNA) at 37 °C for 15 min in D-buffer [10 mM Tris-Cl (pH7.5), 1.5 mM MgCl2, 1 mM CaCl2, 0.25 M sucrose, 0.1 mM PMSF]. The reaction was stopped by the addition of EGTA to a final concentration of 2 mM, and the nuclei were pelleted by centrifugation at 10,000 ×g for 5 min. The pellet was resuspended in N-buffer [10 mM Tris-Cl (pH 6.8), 5 mM EDTA, 0.1 mM PMSF], and dialyzed against N-buffer overnight at 4 °C. The sample was centrifuged at 10,000 ×g for 10 min, and the soluble chromatin supernatant was redialyzed against HA-buffer [0.1 M NaPO4 (pH 6.7), 0.63 M NaCl], and mixed with hydroxyapatite resin (Bio-Rad). After batch binding at 4 °C for 1 h, the resin was packed into a column and washed with 5 volumes of HA-buffer. The core histones were eluted with E-buffer [0.1 M NaPO4 (pH 6.7), 2 M NaCl]. The eluate was applied to a gel filtration column (HiPrep 16/60 S-200, GE Healthcare) to separate the octamer from the H3-H4 tetramer, H2A-H2B dimmer, and other contaminants.

Tail-less core histones were obtained by the partial digestion of nucleosomes with trypsin. The soluble chromatin supernatant was purified as described above. Trypsin was added into the sample to a final concentration of 96 μg/ml, and incubated at 25°C for 7 min. The digestion was stopped by addition of 20mM PMSF and 50ug/ml Aprotinin. The tail-less core histones were isolated by hydroxyapatite chromatography, similar to the purification procedure of normal core histones.

Histone H1 was purified from HeLa cells according to the method developed by A. D. Mirzabekov et al. [38] with slight modifications. The cells were harvested, washed with PBS, and then lysed in 140 mM NaCl, 10 mM Tris-Cl (pH 7.5), and 0.5 % Triton-X100, followed by three washes with the same buffer without the detergent. The nuclei were collected, washed with 0.35 M NaCl, 10 mM Tris-HCl (pH 7.5), and then resuspended in 5 % CCl_3COOH and rotated at 4 °C for 80 min. After centrifugation at 4,000 ×g for 15 min, the soluble histone H1 supernatant was diluted with 10 times the sample volume of Lo-buffer [10 mM Tris-Cl (pH 7.5), 1 mM EDTA, 0.05 % NP-40, and 5 mM 2-mercaptoethanol]. The diluted sample was loaded into a Hi Trap SP column (GE Healthcare) and eluted with a continuous NaCl gradient up to 2 M. The fractions containing the most histone H1 were determined by CBB staining following SDS-PAGE.

Chromatin reconstitution

Equal amounts (0.5 μg) of the purified DNA and the histone octamer were mixed in Hi-buffer [10 mM Tris-Cl (pH 7.5), 2 M NaCl, 1 mM EDTA, 0.05 % NP-40, and 5 mM β-mercaptoethanol], and placed in a dialysis tube (total volume, 50 μl). The dialysis was started in 150 ml of Hi-buffer with stirring at 4 °C. Lo-buffer [10 mM Tris-Cl (pH 7.5), 1 mM EDTA, 0.05 % NP-40, and 5 mM 2-mercaptoethanol] was added to the dialysis buffer at a rate of 0.46 ml/min, and the dialysis buffer was pumped out at the same rate with a peristaltic pump so that the final dialysis

buffer contained 50 mM NaCl after 20 h. The sample was collected from the dialysis tube and stored at 4 °C until used.

In the case of the reconstitution with histone H1, histone H1 was added after the salt dialysis was completed (at the NaCl concentration of 50 mM). The molar ratio of histone H1 to the histone octamer was 1: 1.

For AFM imaging, the reconstituted chromatin solution was fixed with 0.3 % glutaraldehyde for 30 minutes at room temperature. The fixed sample was dropped onto a freshly cleaved mica surface, which was pretreated with 10 mM spermidine. After 10 min incubation at room temperature, the mica was washed with water and dried under nitrogen gas.

AFM observation

AFM observation was performed with a Digital Instruments Multi Mode AFM. All imaging was performed in air using the cantilever tapping mode. The cantilever (OMCL-AC160TS-W2, Olympus) was 129 μm in length with a spring constant of 33-62 N/m. The scanning frequency was 2-3 Hz, and images were captured using the height mode in a 512 x 512 pixel format. The obtained images were plane-fitted and flattened by the computer program supplied in the imaging module.

Calculation of pair potential of nucleosomes from AFM images

Pair potential of nucleosomes was deduced from the analysis of distribution of nucleosomes on the mica surface. Obtained AFM images were analyzed with image

processing software Image J (NIH) to obtain two dimensional (2D) positional information of the center of nucleosomes. We deduced the pair potential $U(r)$ as a function of distance r from the radial distribution function $g(r)$ assuming a Boltzmann distribution, $U(r) = -kT \ln g(r)$, where k is the Boltzmann constant and T is absolute temperature. The radial distribution function in 2D is deduced from the distribution of distances between nucleosomes $N(r)$ with an assumption of equilibrium structure in 2D; $g(r)$ is proportional to $N(r)/r$. Two-dimensional equilibrium structure was previously obtained with a 166-kb DNA chain on a mica surface [39].

3. Results and discussion

Nucleosomes reconstituted with tail-less histones and their physical properties

Partial digestion with trypsin leads to the loss of the tail regions of core histones at the sites shown in Fig. 1A [15]. Mono-nucleosomes purified from HeLa cells [37] were treated with various concentration of trypsin (Fig. 1B), and the partially digested products which had SDS-gel-mobility corresponding to the tail-less subunits (Fig. 1B lane 6) were purified on a hydroxyapatite column [40] (Fig. 1C).

The tail-less core histones were used for nucleosome reconstitution with a 106-kb plasmid [27] and subsequently fixed with glutaraldehyde in buffer containing 50 mM NaCl. (Under this salt concentration, nucleosomes are well spread and easily observed under AFM.) As shown in Fig. 2B and C, tail-less core histones were efficiently incorporated into a nucleosomal array in "beads-on-a-string" structures, similar to normal core histones (Fig. 2A). The efficiency of tail-less nucleosome formation (420 $\pm$ 15 nucleosomes per on 106-kb plasmid; i.e. one nucleosome per 252 bp) was slightly higher than that of normal nucleosome formation (371 $\pm$ 15 nucleosomes per on 106-kb plasmid; i.e. one nucleosome per 286 bp). In both cases of tail-less and normal nucleosomes, the efficiency of nucleosome formation was similar with a physiological density of the nucleosomes; one nucleosome per ~196 bp in higher eukaryotes [41]; i.e. 146 bp nucleosomal DNA and 50 bp linker DNA.

AFM images of long nucleosomal arrays with well-spread individual nucleosomes allowed us to analyze the pair potential of nucleosomes [29]; the distances between nucleosomes were analyzed using an equation for the Boltzmann distribution, yielding the pair potential of nucleosomes (Fig. 2M and N). Fig. 2M shows that the pair potential between nucleosomes containing normal core histones had a minimum at 12.5 nm. In contrast, the pair potential between nucleosomes with tail-less histones is a monotonically decreasing function of distance between the nucleosomes (Fig 2N). These results suggest that nucleosomes consisting of normal core histones attract each other when they are separated by 12.5 nm to 15 nm, and that nucleosomes without tails repel each other. Our data are consistent with previous studies that have proposed a critical role for histone tail in nucleosome-nucleosome attractive interactions; in particular, small angle X-ray scattering experiments using mono-nucleosomes have shown that the attractive interactions between nucleosomes do not manifest in the absence of the tails [42].

Specific behavior of tail-less nucleosomal arrays under conditions in which normal nucleosomal arrays form aggregates

The structures of long nucleosomal arrays show a transition between a spread-out "beads-on-a-string" arrangement and more aggregated states that depend upon the

environmental salt concentrations [13]. Raising the NaCl concentration from 50 mM to 100 mM resulted in huge isotropic aggregates of normal nucleosomes (Fig. 2E). In contrast, tail-less nucleosomes remained in well-spread beads-on-a-string structures at 100 mM NaCl (Fig. 2F-I). This is consistent with previous sedimentation velocity experiments using an array of reconstituted nucleosomes, which have shown that the removal of histone tails prevents the salt dependent condensation of nucleosomes [43].

An analysis of the pair potential revealed that tail-less core histones do not exhibit an attractive potential at the salt concentration of 100 mM (Fig. 2O), similar to their behavior at 50 mM (Fig. 2N). Nucleosomes reconstituted with normal core histones have an attractive force which strengthens with increasing salt concentration, while those with tail-less core histones do not exhibit attraction, and the pair potential does not significantly vary with the salt concentration.

In addition to the salt effect, the histone/DNA ratio in the reconstitution reaction is important for the nucleosome aggregation [29]. Our usual mixing ratio of core histone/DNA has been 1:1 as shown in Fig 2A-I. When the mixing ratio of core histone/DNA was 1.3:1, the reconstituted nucleosomes formed large aggregates (Fig. 2J) as we have reported [29]. In contrast, the nucleosome formation with tail-less histones did not show such a dependency on the histone/DNA ratio (Fig. 2K and L). These results demonstrate that the histone

tails are critical for the structural transition of the nucleosomal array.

It is natural that an increase in the amount of histones does not affect the pair potential between nucleosomes, as shown in Fig.2N and 2P. It may be the same situation for the normal nucleosome (Fig. 2A and 2J), though the pair potential cannot be obtained from the large aggregated structure as in Fig. 2J. The essence in such an aggregated structure as in Fig. 2J is the narrowness in the attractive region (a few nm) of the interaction between nucleosomes; normal nucleosomes, which are dispersed under the attraction approximately equal to thermal fluctuation (1 kT), feel the attractive potential with the increase in the spatial density of nucleosomes and finally become phase-separated into an aggregated and an dispersed states in a single nucleosome array.

Small angle x-ray scattering has demonstrated that an increase in the monovalent salt concentration up to 200 mM enlarges the extension of histone tails [8]. This salt-dependent histone-tail extension has been thought to increase an attractive interaction between the histone tails and DNA or between the histone tails [15], and our work here is consistent with this hypothesis.

Role of histone tails in the linker histone H1-induced chromatin compaction and 30-nm fiber formation.

The addition of histone H1 converts normal nucleosomal arrays reconstituted [13]

or isolated from nuclei [44] into uniform fiber structures with the widths of 20-30 nm under 50-100 mM NaCl (Fig. 3A and B). However, when histone H1 was added into the tail-less nucleosomal array, the uniform fiber was not observed (Fig. 3C and D). It should be noted, however, that even the tail-less nucleosomes are compacted in a zigzag manner in the presence of histone H1 (Fig. 3C and D).

Our finding that the histone tail is required for H1-induced fiber formation but not for H1-induced compaction supports the idea that cooperation between histone tails and linker histone H1 is essential for 30 nm fiber formation. It has been previously reported that the linker histone tails and the tails of histone H3 are redundant for the zigzag arrangement of the nucleosomal array [19]. Thus, perhaps the histone tail plays a role in arranging nucleosomes in a specific manner as a precursor to the formation of a uniform 30nm fiber, but does not play a major role in the interaction between histone H1 and nucleosomes, nor in the compaction of nucleosomes by the addition of H1 [45].

Compaction of nucleosomes due to other chromosomal proteins has been shown to be independent of histone tails. Tail-less nucleosomes can bind to linker histone H1 [45,46], HP1 [47], PC4 (Positive Co-activator 4; transcriptional co-activator [31]), and PARP-1 (Poly (ADP Rybose) Polymerase 1 [48]). In the case of PC4 and PARP-1, AFM observations have revealed that an array of tail-less nucleosomes forms a higher-order structure (irregular-sized aggregation of

nucleosomes) similar to the structure formed by normal histones.

Modifications of core histone tails such as acetylation, phosphorylation and methylation affect the activities of gene expression and duplication [16,17,49], although the physical and structural mechanisms of these effects remain unclear[50]. When the core histone tails were acetylated, the H1-induced fiber became thinner from 30-nm to 20-nm (unpublished data), confirming that histone-tail modification can have dramatic structural effects. Normal core histones have a total of 147 positive charges. These positive charges likely neutralize the negative charges of DNA (2 negative charges per one bp, 292 negative charges per 146 bp nucleosomal DNA). If all acetylation sites [16] are modified, the acetylated core histones possess a total of 117 positive charges that are smaller than those of the unmodified core histones. The tail-less histones have only 95 positive charges, and this charge difference could affect the interaction between nucleosomes. Because tail-less core histones do not possess the positive charges of their normal counterparts, it is likely that they cannot efficiently neutralize the negative charges of the nucleosomal DNA. Tail-less nucleosomes may thus exhibit a stronger electrostatic repulsion between each other and this may prevent tail-less nucleosomes from assembling into fibers, while still allowing compaction into a zigzag array in the presence of histone H1 (Fig. 3F).

4. Conclusion.

The AFM observations shown here suggest a critical role for histone tails in the higher-order folding of the nucleosomal array. The long, normal nucleosomal array reconstituted on 106 kb plasmid shows a structural transition between the well-spread beads-on-a-string and a large aggregation depending on both the environmental salt concentration and the histone/DNA ratio, whereas the tail-less nucleosome array does not form such aggregation under similar conditions. Linker histone H1 converts the array of normal nucleosomes into a 30 nm fiber (Fig. 3A, B, and E), however the tail-less nucleosomes do not form a uniform 30 nm fiber (Fig. 3C, D, and F). Therefore, unlike irregular compaction promoted by PC4 and PARP-1[31,48], H1-induced, well-organized fiber formation requires proper interactions between nucleosomes, that in turn depend on the existence of histone tails.

Acknowledgements:

References

[1]   JD McGhee, G Felsenfeld, Annu Rev Biochem 49 (1980) 1115-56.

[2]   RD Kornberg, Science 184 (1974) 868-71.

[3]   K Luger, AW Mader, RK Richmond, DF Sargent, TJ Richmond, Nature 389 (1997) 251-60.

[4]   PJ Horn, CL Peterson, Science 297 (2002) 1824-7.

[5]   DA Jackson, PR Cook, Int Rev Cytol 162A (1995) 125-49.

[6]   T Owen-Hughes, JL Workman, Crit Rev Eukaryot Gene Expr 4 (1994) 403-41.

[7]   M de Frutos, E Raspaud, A Leforestier, F Livolant, Biophys J 81 (2001) 1127-32.

[8]   S Mangenot, A Leforestier, P Vachette, D Durand, F Livolant, Biophys J 82 (2002) 345-56.

[9]   S Mangenot, E Raspaud, C Tribet, L Belloni, F Livolant, European Physical Journal E 7 (2002) 221-31.

[10]   MH Sato, K Ura, KI Hohmura, F Tokumasu, SH Yoshimura, F Hanaoka, K Takeyasu, FEBS Lett 452 (1999) 267-71.

[11]   J Zlatanova, SH Leuba, K van Holde, Crit Rev Eukaryot Gene Expr 9 (1999) 245-55.

[12]   ME Bianchi, A Agresti, Curr Opin Genet Dev 15 (2005) 496-506.

[13]   K Hizume, SH Yoshimura, K Takeyasu, Biochemistry 44 (2005) 12978-89.

[14]   F Thoma, T Koller, A Klug, J Cell Biol 83 (1979) 403-27.

[15]   C Zheng, JJ Hayes, Biopolymers 68 (2003) 539-46.

[16]   A Kimura, K Matsubara, M Horikoshi, J Biochem (Tokyo) 138 (2005) 647-62.

[17]   SJ Nowak, VG Corces, Trends Genet 20 (2004) 214-20.

[18]   Y Zhang, D Reinberg, Genes Dev 15 (2001) 2343-60.

[19]   SH Leuba, C Bustamante, K van Holde, J Zlatanova, Biophys J 74 (1998) 2830-9.

[20]   SH Leuba, C Bustamante, J Zlatanova, K van Holde, Biophys J 74 (1998) 2823-9.

[21]   KI Hohmura, Y Itokazu, SH Yoshimura, G Mizuguchi, YS Masamura, K Takeyasu, Y Shiomi, T Tsurimoto, H Nishijima, S Akita, Y Nakayama, J Electron Microsc (Tokyo) 49 (2000) 415-21.

[22]   T Sakaue, K Yoshikawa, SH Yoshimura, K Takeyasu, Phys Rev Lett 87 (2001) 078105.

[23]   MA Karymov, M Tomschik, SH Leuba, P Caiafa, J Zlatanova, Faseb J 15 (2001) 2631-41.

[24]   GR Schnitzler, CL Cheung, JH Hafner, AJ Saurin, RE Kingston, CM Lieber, Mol Cell Biol 21 (2001) 8504-11.

[25]   K Hizume, SH Yoshimura, H Maruyama, J Kim, H Wada, K Takeyasu, Arch Histol Cytol 65 (2002) 405-13.

[26]   JG Yodh, N Woodbury, LS Shlyakhtenko, YL Lyubchenko, D Lohr, Biochemistry 41 (2002) 3565-74.

[27]   K Hizume, SH Yoshimura, K Takeyasu, Cell Biochem Biophys 40 (2004) 249-62.

[28]   E Davies, KS Teng, RS Conlan, SP Wilks, FEBS Lett 579 (2005) 1702-6.

[29]   T Nakai, K Hizume, SH Yoshimura, K Takeyasu, K Yoshikawa, Europhysics Letters 69 (2005) 1024-30.

[30]   Y Yoshikawa, K Hizume, Y Oda, K Takeyasu, S Araki, K Yoshikawa, Biophys J 90 (2006) 993-9.

[31]   C Das, K Hizume, K Batta, BR Kumar, SS Gadad, S Ganguly, S Lorain, A Verreault, PP Sadhale, K Takeyasu, TK Kundu, Mol Cell Biol 26 (2006) 8303-15.

[32]   K Hizume, S Araki, K Yoshikawa, K Takeyasu, Nucleic Acids Res 35 (2007) 2787-99.

[33]   FJ Solis, R Bash, H Wang, J Yodh, SA Lindsay, D Lohr, Biochemistry 46 (2007) 5623-34.

[34]   M Ikeno, H Inagaki, K Nagata, M Morita, H Ichinose, T Okazaki, Genes Cells 7 (2002) 1021-32.

[35]   B Vissel, KH Choo, Nucleic Acids Res 19 (1991) 271-7.

[36]   H Shizuya, B Birren, UJ Kim, V Mancino, T Slepak, Y Tachiiri, M Simon, Proc Natl Acad Sci U S A 89 (1992) 8794-7.

[37]   TE O'Neill, M Roberge, EM Bradbury, J Mol Biol 223 (1992) 67-78.

[38]   AD Mirzabekov, DV Pruss, KK Ebralidse, J Mol Biol 211 (1990) 479-91.

[39]   N Yoshinaga, K Yoshikawa, S Kidoaki, Journal of Chemical Physics 116 (2002) 9926-29.

[40]   RH Simon, G Felsenfeld, Nucleic Acids Res 6 (1979) 689-96.

[41]   JL Compton, M Bellard, P Chambon, Proc Natl Acad Sci U S A 73 (1976) 4382-6.

[42]   A Bertin, A Leforestier, D Durand, F Livolant, Biochemistry 43 (2004) 4773-80.

[43]   M Garcia-Ramirez, F Dong, J Ausio, J Biol Chem 267 (1992) 19587-95.

[44]   F Thoma, T Koller, J Mol Biol 149 (1981) 709-33.

[45]   LM Carruthers, JC Hansen, J Biol Chem 275 (2000) 37285-90.

[46]   W An, J Zlatanova, SH Leuba, K van Holde, Biochimie 81 (1999) 727-32.

[47]   AL Nielsen, M Oulad-Abdelghani, JA Ortiz, E Remboutsika, P Chambon, R Losson, Mol Cell 7 (2001) 729-39.

[48]   DA Wacker, DD Ruhl, EH Balagamwala, KM Hope, T Zhang, WL Kraus, Mol Cell Biol 27 (2007) 7475-85.

[49]   C Martin, Y Zhang, Nat Rev Mol Cell Biol 6 (2005) 838-49.

[50]   M Garcia-Ramirez, C Rocchini, J Ausio, J Biol Chem 270 (1995) 17923-8.
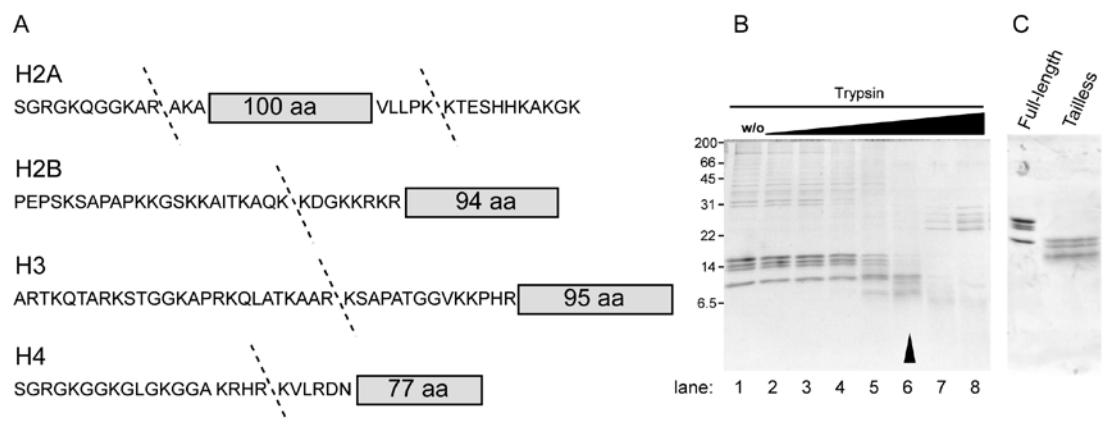
Figure captions

Fig. 1   Partial digestion of histone tail regions   (A) amino acid sequence of tail regions of core histone subunits. The dotted lines indicate the sites of digestion due to treatment with trypsin, as reported in [15]. (B) Mono-nucleosomes were purified from MNase digested HeLa nuclei were treated with various amount of trypsin, and run in SDS-polyacrilamide gel. Proteins were detected by CBB staining. (C) After the treatment with (right lane) or without (left lane) trypsin, core histones were purified by hydroxylapatite chromatography, and run in SDS-polyacrilamide gel. Proteins were detected by CBB staining.

Fig. 2   AFM images of the reconstituted nucleosomal array. Normal core histones (A) or tail-less core histones (B and C) were mixed with 106-kb plasmid in the buffer containing 2 M NaCl and then dialyzed against the buffer containing lower concentration of NaCl. Dialysis was stopped at a final NaCl concentration of 50 mM, and samples were fixed with 0.3% glutaraldehyde. Samples were then mounted on a cleaved mica surface pre-treated with 10 mM spermidine, washed with distilled water, dried under nitrogen gas, and observed by AFM. (D-I) Nucleosomes were reconstituted from 106-kb plasmid and normal (D and E) or tail-less core histones (F-I). Nucleosome reconstitution was performed as before, and then the samples were additionally dialyzed against buffer containing 100 mM
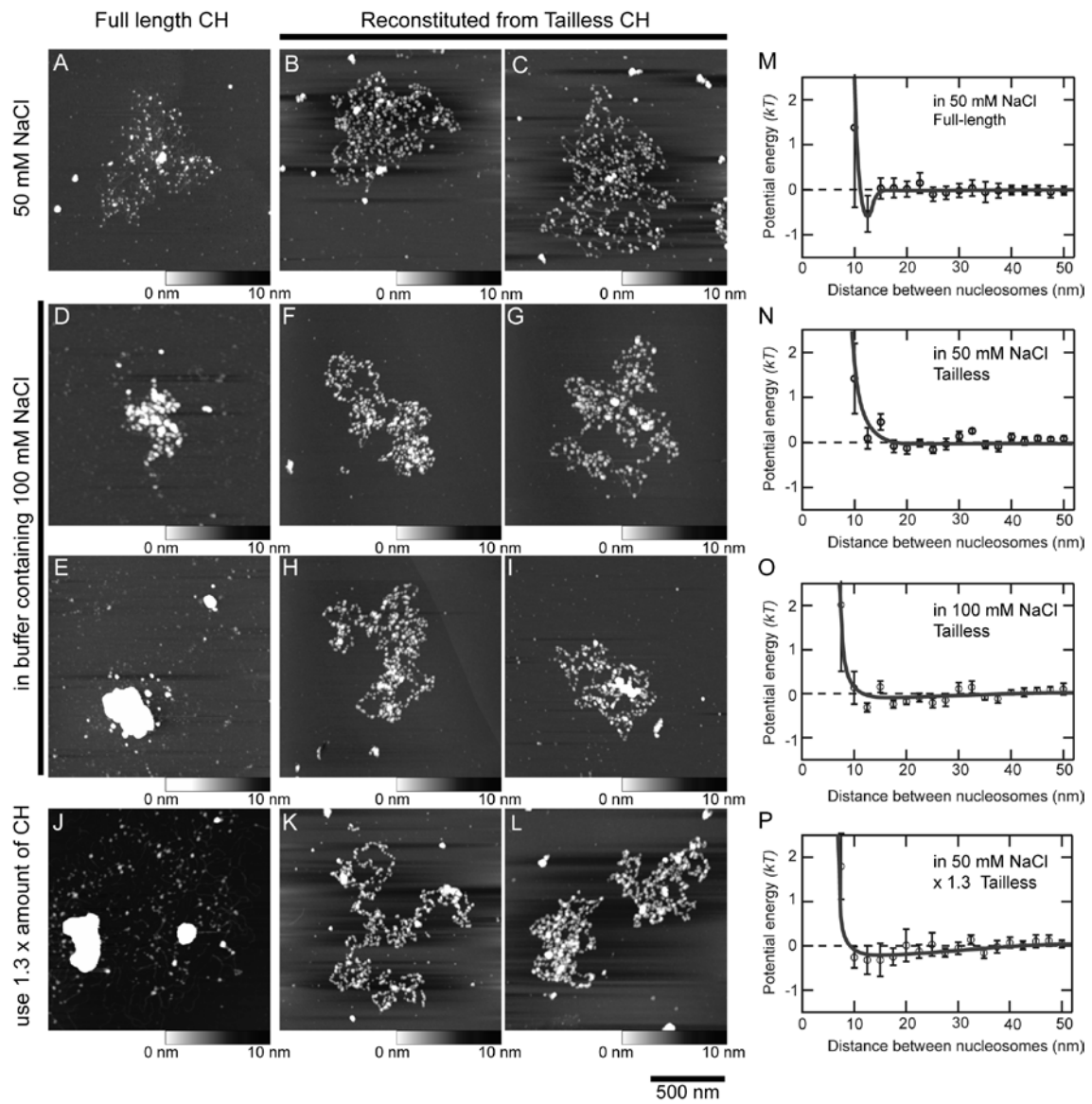
NaCl. After this dialysis step, the reconstituted samples were fixed and prepared for imaging as previously described. (J-L) Nucleosomes were reconstituted from 106-kb plasmid and normal (J) or tail-less core histones (K and L). Core histones were used $1.3\times$ amount of the experiments shown in Fig. 2 A-I. (M-P) The pair potential of nucleosomes obtained by an equation for the Boltzmann distribution. Nucleosomes were reconstituted under the condition in which the AFM images of nucleosomes are shown in panel A (M), B and C (N), F-I (O), or K and L (P), respectively.

Fig. 3　Linker-histone H1 induces higher-order structure. (A-D) AFM images of reconstituted chromatin fibers. Nucleosomes were reconstituted from 106-kb plasmid and normal (A and B) or tail-less core histones (C and D), and linker histone H1 was added into the nucleosomal array. (E and F) Schematic illustrations of uniformed H1-induced fiber reconstituted from normal nucleosomes (E) and disorderd zig-zag aggregation reconstituted from tail-less nucleosomes (F).

A

H2A
SGRGKQGGKAR AKA [100 aa] VLLPK KTESHHKAKGK

H2B
PEPSKSAPAPKKGSKKAITKAQK KDGKKRKR [94 aa]

H3
ARTKQTARKSTGGKAPRKQLATKAAR KSAPATGGVKKPHR [95 aa]

H4
SGRGKGGKGLGKGGA KRHR KVLRDN [77 aa]

B

Trypsin

w/o

200-
66-
45-
31-
22-
14-
6.5-

lane: 1 2 3 4 5 6 7 8

C

Full-length
Tailless

Hizume et al.   Fig. 1

23

Full length CH

Reconstituted from Tailless CH

50 mM NaCl

A

B

C

0 nm   10 nm   0 nm   10 nm   0 nm   10 nm

in buffer containing 100 mM NaCl

D

F

G

0 nm   10 nm   0 nm   10 nm   0 nm   10 nm

E

H

I

0 nm   10 nm   0 nm   10 nm   0 nm   10 nm

use 1.3 x amount of CH

J

K

L

0 nm   10 nm   0 nm   10 nm   0 nm   10 nm

500 nm

M

in 50 mM NaCl
Full-length

Potential energy (kT)
Distance between nucleosomes (nm)

N

in 50 mM NaCl
Tailless

Potential energy (kT)
Distance between nucleosomes (nm)

O

in 100 mM NaCl
Tailless

Potential energy (kT)
Distance between nucleosomes (nm)

P

in 50 mM NaCl
x 1.3 Tailless

Potential energy (kT)
Distance between nucleosomes (nm)

Hizume et al.   Fig. 2

24

Full length CH   Tailless CH

fiber   disordered zig-zag

Hizume et al.   Fig. 3